Environmental Science Nano

PAPER

View Article Online
View Journal | View Issue

Cite this: *Environ. Sci.: Nano*, 2017, 4, 2010

Carbon-nanotube sponges enabling highly efficient and reliable cell inactivation by low-voltage electroporation†

Zheng-Yang Huo,[a] Yufeng Luo,[bc] Xing Xie,[d] Chao Feng,[e] Kaili Jiang,[b] Jiaping Wang *[b] and Hong-Ying Hu *[af]

Received 21st June 2017,
Accepted 15th August 2017

DOI: 10.1039/c7en00558j

rsc.li/es-nano

The recent bloom of nanomaterials has kindled a strong demand for new cell inactivation technology that can replace the conventional cell inactivation process with high throughput, free chemicals usage and outstanding efficacy to all pathogens to overcome the critically global issue, *i.e.* microbial infection. Herein, we construct a macroscopic carbon nanotube (CNT) sponge using a simple self-assembly method. Based on the technology of 1D nanostructure assisted electroporation, an electroporation disinfection cell (EDC) equipped with CNT sponge achieved superior cell inactivation performance (<0.00001% microbe survival rate) within a contact time of 5 s at an extremely low applied voltage (2 V), trace energy consumption (20 J L^{-1}) and outstanding durability (>60 min). The CNT sponge EDC can be easily powered by batteries or solar cells and shows the best energy consumption performance among all the cell inactivation technologies. Cell inactivation using the CNT sponge EDC has significant potential for practical applications.

Environmental significance

Pathogenic infection, one of the most serious public issues, causes the death of millions of people every year. Traditional water disinfection methods (*e.g.*, chlorination and ultraviolet radiation) include concerns about the formation of carcinogenic disinfection by-products, pathogen reactivation and/or excessive energy consumption. This study provides a new disinfection method based on the technology of 1D nanostructure assisted electroporation. An electroporation disinfection cell (EDC) was fabricated equipped with macroscopic carbon nanotube (CNT) sponges. This CNT sponge EDC provided a new approach to achieve superior cell inactivation performance (<0.00001% microbe survival rate) within a short contact time of 5 s at an extremely low applied voltage (2 V) for long-time reliable application.

1. Introduction

With the blooming practical demands of life and biological science, the development of highly-efficient and reliable operational devices assisted by nanomaterials has attracted more and more attention.[1–4] Among all the recently studied nanomaterials, carbon nanotube (CNT) has been explored intensively due to its high electrical conductivity (10^5 S cm^{-1}), large thermal conductivity (6000 W m^{-1} K) and superior mechanical properties.[5,6] In order to take these advantages in practical devices, CNTs are usually required to be assembled into macroscopic architectures with the aid of organogelators (*e.g.*, surfactants and polyvinyl alcohol).[7–10] However, in this structure, CNTs are glued by an organic binder, which inevitably reduces the physical durability and surface activity.[7,8,10–12] In our recent study, instead of organogelator modification, we first reported a macroscopic CNT sponge using a simple strategy. When soaked in a piranha (mixed H_2SO_4 and H_2O_2) solution, the super-aligned CNT (SACNT) films would spontaneously expand into a sponge shape and after cryodesiccation an ultra-light and three-dimensional pure carbon nanotube (CNT) aerogel was synthesized. This new CNT sponge achieved high porosity (99.95%), high specific surface area (298 m^2 g^{-1}) and chemical stability, which showed great potential for oil adsorption (1389 mg mg^{-1} for phenixin; highest value reported in the literature) and other practical applications.[13]

[a] *Environmental Simulation and Pollution Control State Key Joint Laboratory, State Environmental Protection Key Laboratory of Microorganism Application and Risk Control (SMARC), School of Environment, Tsinghua University, Beijing 100084, PR China. E-mail: hyhu@tsinghua.edu.cn, hyhu-edu@mail.tsinghua.edu.cn; Tel: +86 10 6279 4005*
[b] *Department of Physics and Tsinghua-Foxconn Nanotechnology Research Center, Tsinghua University, Beijing 100084, PR China. E-mail: jpwang@tsinghua.edu.cn*
[c] *Department of Materials Science and Engineering, Tsinghua University, Beijing 100084, PR China*
[d] *School of Civil and Environmental Engineering, Georgia Institute of Technology, Atlanta, Georgia 30332, USA*
[e] *Institute for Advanced Study, Tsinghua University, Beijing 100084, PR China*
[f] *Shenzhen Environmental Science and New Energy Technology Engineering Laboratory, Tsinghua-Berkeley Shenzhen Institute, Shenzhen 518055, PR China*
† Electronic supplementary information (ESI) available. See DOI: 10.1039/c7en00558j

Among all these outstanding features, inside its three-dimensional (3D) continuous internal surface, our CNT sponge also offered plenty of nanoscaled tip structures that have unique biological[14–17] and electronic properties (*e.g.*, field emission, large surface area and high conductivity),[18–20] which may have specific interactions with bacteria (*e.g.*, promote control or inhibit their microbial activities).[20,21] According to the simulation results, if applied using a relatively low voltage, an enhanced electric field ($\sim 10^7$ V m^{-1}) can be built up near the tip structure.[22] When the cell is exposed to a sufficiently high electric field, a rapid and large increase in the electric conductivity and permeability of the biological membranes may occur.[23] The physical mechanism of electroporation is already an established technique in several areas of medicine and promising to be an alternative to traditional cell inactivation methods (thermal, chlorine and ultraviolet radiation) due to its typical competitive advantages such as high throughput,[24,25] free chemicals usage[23,25] and outstanding efficacy to all pathogens.[25] However, concerns about the high energy consumption (>10 kJ per liter of liquid sample treated) and safety issues to generate a strong field ($\sim 10^7$ V m^{-1}) have been the major obstacles to the large-scale implementation of electroporation for cell inactivation.[23,26]

Taking advantage of the special electric field enhancement property, the electric field near the tip structure can be several orders of magnitude stronger. Even with a low applied voltage, the electric field near the tip structure can still be strong enough to cause irreversible electroporation. On the basis of this phenomenon, one-dimensional (1D) nanostructure (*e.g.*, nanowire and nanotube) assisted electroporation disinfection has been reported in several studies.[17,27,29,31] However, the voltages applied in these studies are still higher than the typical voltages used for water electrolysis (>2 V). Thus, one concern about this new disinfection process is that water electrolysis may lead to the formation of chlorination disinfection by-products. Another concern is the durability of the 1D nanostructure. Considering that the typically implemented 1D nanostructures are metal or metallic oxide (*e.g.*, Ag, ZnO, CuO), it is not clear whether 1D nanostructure assisted electroporation can work for long-term treatment with an applied voltage.

Herein, we have prepared a pure CNTs sponge using a simple self-assembly method. A massive amount of CNT tips were rooted on the CNT sponge's 3D continuous internal surface (Fig. 1a) providing an extremely strong electric field (Fig. 1b), which can be used to achieve electroporation cell inactivation with low applied voltages and sufficient reaction sites for cell inactivation (Fig. 1c). A new electroporation-disinfection cell (EDC) equipped with such unique CNT sponges (Fig. 2) achieved superior cell inactivation performance with an extremely low applied voltage and energy consumption. This novel cell inactivation process is promising for practical food, water and medical waste treatment.

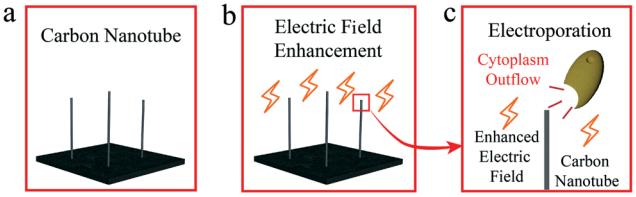

Fig. 1 Schematics showing the mechanism of carbon-nanotube sponges enabling cell inactivation *via* low-voltage electroporation. (a) CNT sponges with considerable tip structure. (b) CNT sponges with a low applied voltage. The yellow lightenings show the electric field strength enhanced by the CNT (not quantified). (c) Bacteria are electroporated and inactivated due to the strong electric field.

2. Materials and methods

2.1 Fabrication of carbon nanotube (CNT) sponge and the construction of an electroporation disinfection cell (EDC) device

The procedure used for the synthesis of CNT sponges has been reported in previous studies.[13] A SACNT film was placed in piranha solution (98 wt% H_2SO_4 and 35 wt% H_2O_2 at a volume ratio of 7 : 3) and expanded spontaneously into a CNT sponge. After a few days, the CNT sponge was repeatedly rinsed with deionized water until the pH value reached 7. The CNT sponge was then transferred into a beaker or a petri dish for the following freeze-drying process using freeze drying equipment (Four-Ring, LGD-10D) and then cut into the desired size (diameter of 1 cm and thickness of 0.5 cm). The cylinder CNT electrodes were then placed into a Plexiglass coaxial electrode holder (5 cm × 5 cm × 2.5 cm) with a plastic mesh (~100 μm) in the middle to prevent short circuit. Field emission scanning electron microscopy (FE-SEM) images were taken on a FEI Sirion 200 microscope at an operating voltage of 10 kV.

2.2 Total chlorine and current measurement

The total chlorine concentrations in both the control and treated samples were measured with a Hanna HI96724 total chlorine pocket colorimeter. The voltages applied to the EDC were provided using a direct current power supply (DG1718E-5). The anode of the power supply was connected to one electrode and the cathode to the other. During the EDC treatment, the water samples were passed through the electrodes and certain voltages were applied to those two electrodes. The current in the circuit was measured using a digital multimeter (UNI-T UT39C).

2.3 Bacteria and virus inactivation with the EDC

Escherichia coli (ATCC 15597), *Enterococcus faecalis* (ATCC 19433) and *Bacillus subtilis* (ATCC 6633) were cultured to the log phase (12 h) and then diluted into desired solutions of $\sim 10^7$ CFU mL^{-1}. Each water sample (50 mL) was flowed through the EDC equipped with the prepared CNT sponges at different contact times. At the same time, a voltage of 2 V was applied to the device. The control samples were passed

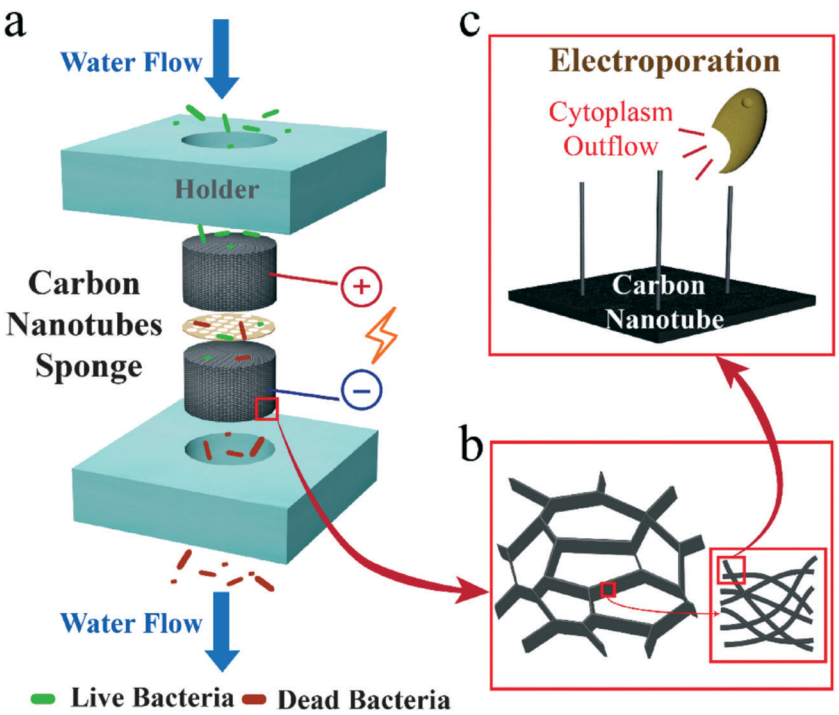

Fig. 2 Fabrication and characterization of the electroporation disinfection cells (EDCs) with CNT sponge electrodes. Schematics showing (a) the construction of the EDC, (b) the macroporous structure of the CNT sponges electrodes and (c) the electroporation cell inactivation mechanism.

through the same EDC device at the same flow rate without an applied voltage, investigating the adsorption or interception phenomenon of the CNT sponge (Fig. S1†). All the effluents were collected in sterilized centrifugal tubes. The bacterial concentrations of the effluents were measured using standard spread plating techniques. Each sample was serially diluted and then plated in duplicate and incubated at 37 °C for 24 h. The virus, bacteriophage MS2, was grown with the *E. coli* host on a shaker table set to 150 rpm at 37 °C for 24 h. MS2 was isolated and concentrated using the polyethylene glycol (PEG) precipitation method. A solution of $\sim 10^3$ PFU mL^{-1} was prepared using normal saline solution (9.0 g L^{-1} sodium chloride). MS2 was enumerated using a double agar layer method. All plating was carried out within 3 h of the filtration experiment. The treated and control samples were compared to determine the inactivation efficiency. All plating was carried out within 3 h of the disinfection experiment. The treated and control samples were compared to determine the inactivation efficiency.

2.4 Bacteria sample preparation for scanning electron microscopy (SEM)

The pretreatment process used for all the samples was as follows: (1) both the control and treated samples were treated by EDC at 2 V for 10 s and were harvested by centrifugation at 14 500 rpm for 15 min (HITACHI RX2 series) and the supernatants were removed. All the samples were fixed overnight in fixative containing 0.1 M phosphate buffered solution (pH 7.3), 2% glutaraldehyde and 4% paraformaldehyde at 4 °C, then washed with DI water for 5 min; (2) the samples were then secondary fixed in 1% osmium tetroxide at 4 °C for 1–2 h, followed by washing with DI water for 10 min; (3) the samples were dehydrated in increasing concentrations of ethanol solution (50, 70, 90 and 100%) and critical point dried in 100% ethanol with liquid CO_2 and (4) the samples were finally sputter coated with 10 nm of gold. All the SEM images were recorded on a field emission scanning electron microscope (FEI XL30 Sirion SEM).

2.5 Live/dead baclight staining experiment

The control and treated samples treated by EDC at 2 V for 10 s were harvested by centrifugation at 14 500 rpm for 15 min (HITACHI RX2 series) and the supernatants were removed. The samples were re-suspended in 0.1 M phosphate buffered solution (pH 7.3) to 100 μL. A Live/Dead Baclight kit (Molecular Probes®) was used to implement the staining experiment. Equal volumes (2.5 μL) of SYTO 9 (0.6 mM) and PI (3 mM) dye solutions were added into the samples. The samples were stored in the dark for 30 min and examined using fluorescent microscopy.

2.6 Bacteria DNA concentration measurement

10 mL of the *E. coli* samples (10^9 CFU mL^{-1}) were treated by EDC at 2 V for 5 min in a flask. Then, the electrodes and *E. coli* samples were treated by ultrasonication for 30 min to extract the DNA from the cells, harvested by centrifugation at 14 500 rpm for 15 min (HITACHI RX2 series) and supernatants were used to measure the DNA concentration. 100 μL of

the supernatant was added to 2.5 mL of 4,6-diaminodino-w-phenylindole (DAPI) reagent (0.2 ppm DAPI in 100 mM NaCl, 10 mM EDTA, 10 mM TRIS, pH 7). The samples were measured using a microplate reader (Molecular Devices™ SpectraMax) (excitation wavelength fixed at 360 nm).

2.7 Electric field simulation

Electric field simulations were conducted using commercial Matlab2014 software. The electric field in the vicinity of the CNT tip was simulated. The distance between the electrodes and the applied voltage between the two electrodes were 200 μm and 2 V, respectively. The density of the CNT tip distribution was 100 per μm^2 and the CNT diameter was 10 nm.

3. Results and discussion

3.1 Fabrication and characterization of the CNT sponge electroporation disinfection cells (EDCs)

The CNT sponges were prepared as described in our earlier publication.[13] An SACNT sheet was continuously drawn from an SACNT array on a silicon wafer and then rolled into a unidirectional multilayer film with 200 layers (Fig. S1a†). The as-prepared SACNT film was then placed in piranha solution (98 wt% H_2SO_4 and 35 wt% H_2O_2 at a volume ratio of 7 : 3) and began to self-expand spontaneously (Fig. S1b†) and finally formed a large 3D continuous sponges structure (Fig. S1c†). Macroscopic CNT sponges with the desired shape and density (Fig. 3a and b) could be obtained by controlling the size of the original CNT film, immersion time and shape of the containers during the self-expansion process. A massive amount of CNT tips were rooted continuously on the 3D macroporous sponge structure (Fig. 3c, d and e) with a pore size varied from 200 to 400 μm (Fig. 3f).

An EDC was built by placing two pieces of the CNT sponge electrodes (with a diameter of 1 cm and thickness of 0.5 cm) in a plexiglass coaxial electrode holder (5 cm × 5 cm × 2.5 cm) (Fig. 2, S1d and e†). For electroporation-based cell inactivation, the CNT sponge electrode revealed obvious advantages. The continuous 3D macroscaled porous structure (diameter >200 μm) allowed water to easily flow through with little hydraulic resistance. Considering the large pore size, the CNT sponge was unlikely to be clogged by the microbes with water flow according to the investigation of the adsorption phenomenon of CNT sponge (Fig. S2†). Without an applied voltage, the bacteria solution was flowed through the CNT sponge and after 60 min the bacteria concentrations at the inlet and effluent were similar (Fig. S2a†) without cell attachment on the CNT sponge (Fig. S2b and c†). Moreover, the complex flowing pattern within the porous increased the opportunity for microbes to approach the electrode surface where the electric field was significantly enhanced by the CNT tips and electroporation cell inactivation occurred. The large pores with sizes of several hundred micrometers were unlikely to be clogged by the microbes, which were normally <10 μm in size. Because massive amount of CNTs were rooted on the macroscale porous structure by *in situ* self-expansion, there were plenty of electroporation cell inactivation sites and the physical contact of CNTs was stable and the electrical connection was guaranteed.

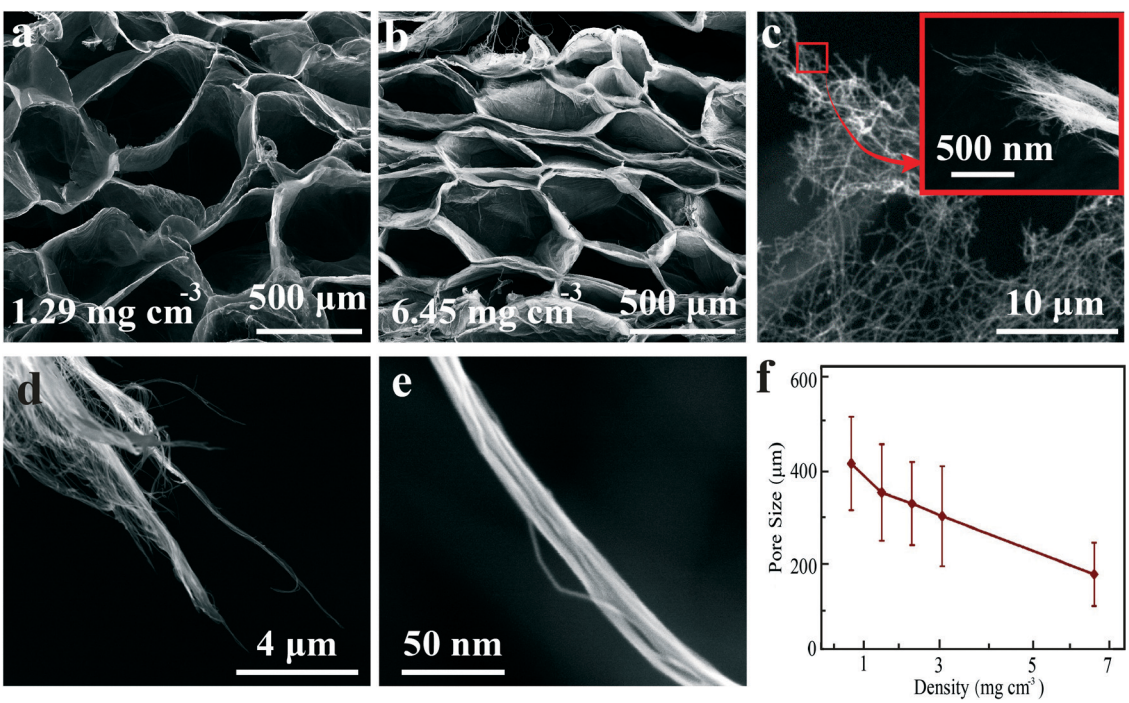

Fig. 3 SEM images of the CNT sponge with low (a) and high (b) density. (c and d) SEM images showing the CNT tips rooted on the 3D continuous macrostructure of the wall of the CNT sponges. (e) SEM image of a single CNT rooted on the CNT sponge. (f) The densities of the CNT sponges corresponding to different pore sizes.

3.2 Cell inactivation performance and energy efficiency of the CNT sponge EDC

To investigate the cell inactivation efficacy of our CNT sponge, we performed the low-voltage electroporation using the electroporation disinfection cell by treating the *E. coli* samples ($\sim 10^7$ CFU ml^{-1}; C_{in}, concentration in the influent) passing vertically through the electrodes with the desired flow rate and applied voltage (2 V). The *E. coli* concentrations in the effluent (C_{eff}) were carefully analyzed using a cultivation method and the survival rates were calculated [$E = C_{eff}/C_{in}$]. As shown in Fig. 4a, the inactivation efficiency generally increased with the CNT sponge density and contact time. When the density was 1.29 mg cm^{-3}, ~0.01% *E. coli* could survive after 20 s of CNT sponge EDC treatment. Increasing the density to 3.225 and 6.45 mg cm^{-3} effectively increased

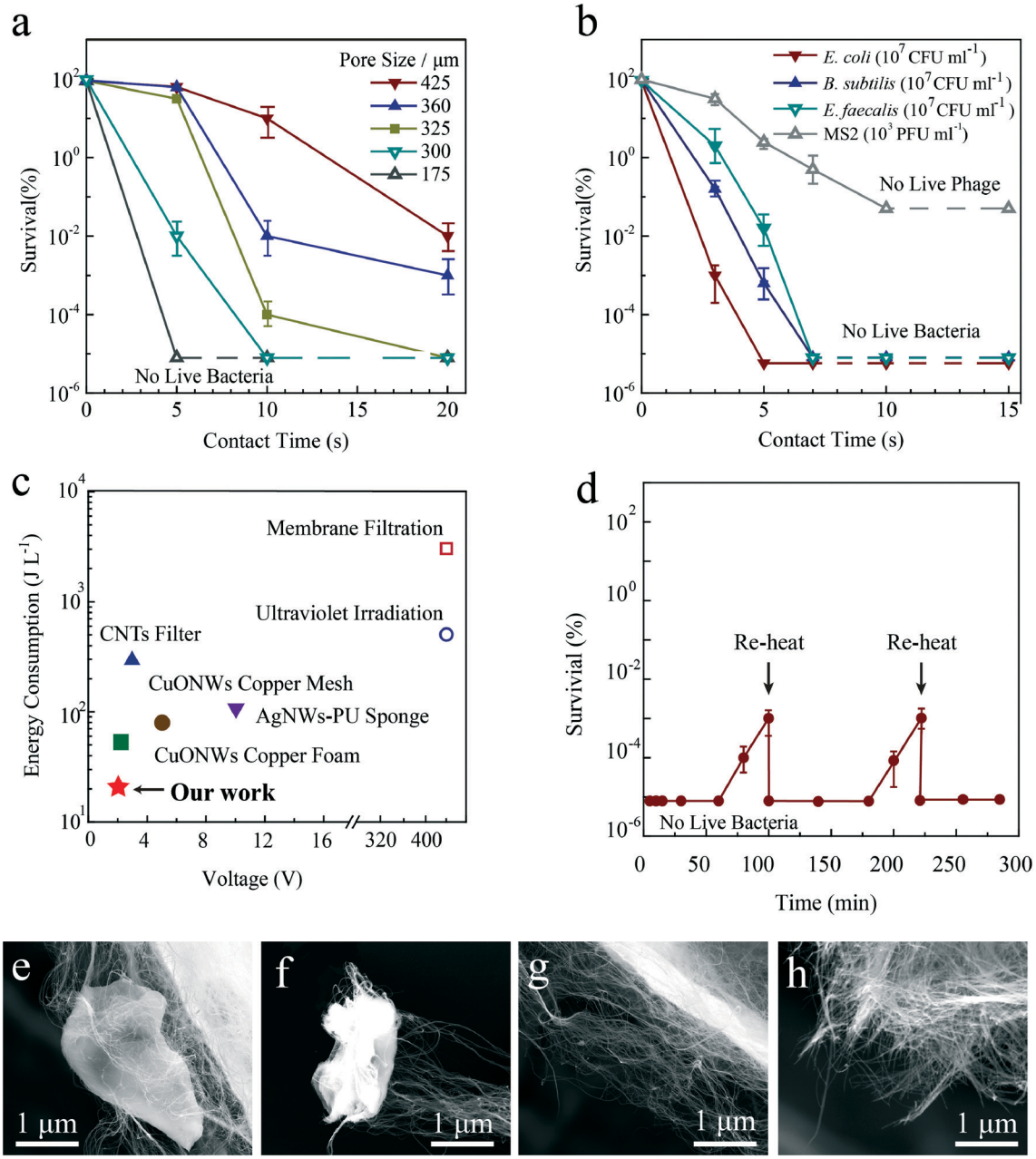

Fig. 4 Cell inactivation performance and energy efficiency of the CNT sponge EDC. (a) The removal efficiencies of *E. coli* treated with the CNT sponge EDC with different densities with an applied voltage of 2 V at different contact times. (b) The survival rate of *E. coli*, *B. subtilis*, *E. faecalis* and MS2 varied with contact time under an applied voltage of 2 V. The dashed lines indicate that all microbes were inactivated and no live microbes could be detected. (c) A comparison of the energy consumption of the CNT sponge EDC with recently reported advanced cell inactivation methods. (d) The durability evaluation of the CNT sponge EDC. (e and f) SEM characterization of the CNT sponge filter after long-term (60 min) use. The bacteria were attached on the tip structure of the CNT. (g and h) SEM characterization of the CNT sponge filter after regeneration. No cell attachment was observed.

the cell inactivation efficiency with an *E. coli* survival rate of <0.00001% (indicating no detection of *E. coli* in the effluent) and lowered the contact time required to achieve complete cell inactivation performance to 10 and 5 s, respectively. Moreover, the other three model microorganisms studied including two Gram-positive bacteria, *Bacillus subtilis* and *Enterococcus faecalis*, and a bacteriophage, MS2 (Fig. 4b) were treated using a 2 V EDC equipped with the CNT sponges (density 6.45 mg cm^{-3}). Less than 0.00001% of both *B. subtilis* and *E. faecalis* survived (indicating no detection of bacteria in the effluent) when the contact times were longer than 7 s, which was similar to the inactivation performance seen for *E. coli* (Gram-negative). The slightly larger dose required to effectively kill Gram-positive bacteria was probably due to the thicker layer of peptidoglycan on the cell membrane. No live MS2 could be detected after 20 s of CNT sponge EDC treatment.

To investigate the energy consumption and potential health risk from the formation of carcinogenic disinfection by-products (DBPs), the currents in the circuit and total chlorine concentrations in the effluent were measured for the EDC treated *E. coli* samples ($\sim 10^7$ CFU mL^{-1}; 9.0 g L^{-1} sodium chloride). The contact time was fixed at 5 s, corresponding to the fastest flow rate for complete inactivation after a 2 V treatment and the applied voltages were varied from 0 to 5 V. When the applied voltages were less than 2 V, the currents were minimal (<2 mA), indicating little electrochemical reaction (Fig. S3†). No chlorine was detected in the effluent, which suggested that chlorine disinfection was not the mechanism for *E. coli* inactivation during the treatment process. In addition, without chlorine generation, the potential for DBP formation was extremely low. When the applied voltages were larger than 2 V, the currents increased notably. At 5 V, the current was 45 mA, more than 25 times that at 2 V (1.7 mA). Water decomposition started along with bubble formation. Meanwhile, chlorine was generated because of the oxidation of chloride and the concentrations increased in proportion to the current. When the applied voltage was increased to 5 V, 0.4 mg L^{-1} total chlorine was detected in the effluent. These results suggested that applying a voltage less than 2 V significantly reduced the extent of the electrochemical reaction and chlorine generation during electroporation and cell inactivation, and thus avoided the formation of DBPs and lowered the health risks. At the same time, with less water decomposition, the level of energy consumption of the EDC was reduced to 20 J for treating 1 L of water *via* a treatment at 2 V for 5 s. This value was significantly lower than that of UV disinfection ($\sim 1 \times 10^3$ J L^{-1}) and membrane filtration ($\sim 1 \times 10^4$ J L^{-1})[28] and less than other nanomaterial assisted disinfection technologies reported in previous studies (>100 J L^{-1})[22,29–32] (Fig. 4c).

Moreover, the durability of the CNT sponge EDC is relatively high due to its self-assembly synthesis mechanism (Fig. 4d). Even after 60 min of continuous treatment, the CNT sponge could achieve complete cell inactivation and after that cell blocking began to occur. SEM characterization of the CNT sponge filter after long term (60 min) use (Fig. 4e and f) showed that the bacteria tended to attach on the tip structure of the CNT. The CNT enhanced electric field for electroporation disinfection only existed within several μm of the tip structure. Thus, these attached bacteria may repel others cell getting into the on electroporation zone and lead to a failure of disinfection. However, after heating the blocked electrodes at 400 °C for 10 min, the CNT sponge was recovered by removing the attached bacteria and the cell inactivation efficiency could be guaranteed for another 60 min of continuous treatment. After several treatment-recovery cycles, all the cells could be killed indicating the prominent high disinfection durability of the CNT sponge. From all the results above, such a low level of energy consumption and high durability could be easily provided by batteries and solar cells, making the CNT sponge EDC very promising for practical applications. A commercial alkaline battery can treat at least 300 L of water in only 25 min with the help of a 100 cm^3 CNT sponge that was matured for large scale synthesis.

3.3 Confirmation of the electroporation cell inactivation mechanism of the CNT sponge EDC

SEM images confirmed the mechanism of electroporation cell inactivation for the CNT sponge EDC. When compared to untreated *E. coli* whose cell membranes are complete and smooth (Fig. 5a), the treated *E. coli* (2 V, 10 s) had obvious electroporation holes on their surface (Fig. 5b), indicating lethal membrane damage. The results of a staining test with the Live/Dead Baclight kit (Fig. 5c and d) also suggested that the *E. coli* cells lost their membrane integrity during the treatment because Syto 9 entered all the cells despite the membrane integrity and PI entered only the cells with a damaged membrane. Moreover, due to the membrane damage caused by electroporation, the DNA in the cells also flowed out. When compared with the untreated cell sample, a notable amount of DNA was released into the water after treatment at 2 V for 3 s. Increasing the contact time from 3 to 30 s significantly enhanced the DNA release, indicating severe electroporation membrane damage (Fig. 5e).

To enhance the electric field strength, the CNTs were introduced in this study based on the theory of the "lightening rod effect". When a metallic rod was inserted into a region of a uniform electric field, the electric field strength near the tip (E_{tip}) of the metallic rod can be enhanced by a degree roughly estimated by eqn (1) and (2):

$$\frac{E_{tip}}{E_0} = \alpha \cdot \frac{l_{rod}}{d_{rod}} \quad (1)$$

$$E_0 = \frac{U}{d} \quad (2)$$

where E_0 is the strength of the original uniform electric field, α is a constant, l_{rod} is the length of the rod and d_{rod} is the

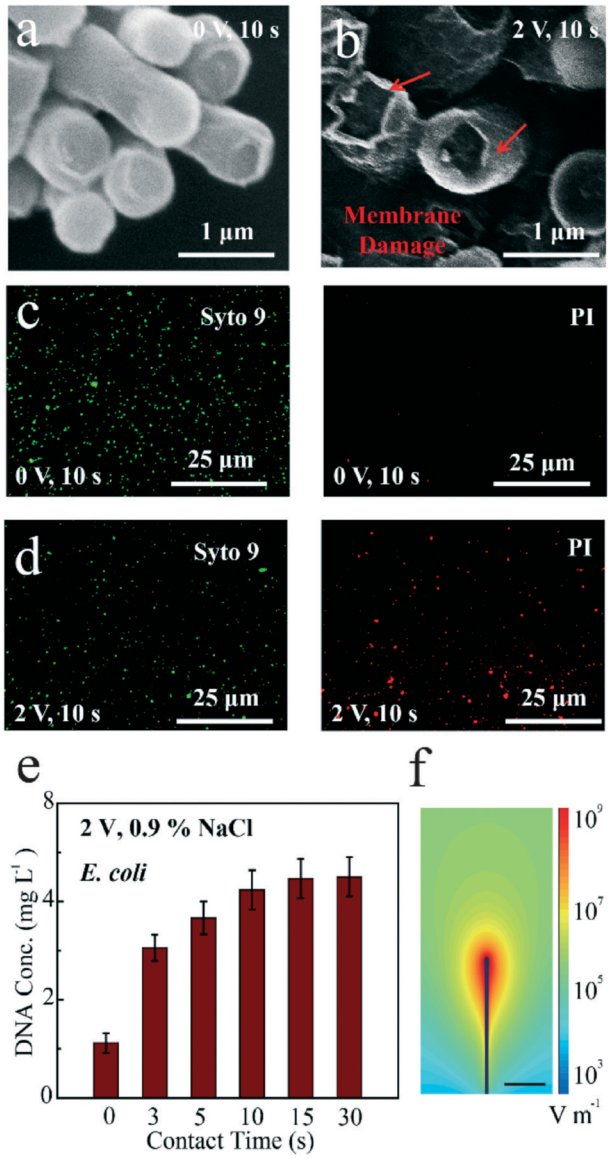

Fig. 5 Electroporation evidence: SEM images, dye staining results, released DNA concentration and electric field distribution. (a) SEM image showing the morphologies of *E. coli* without any treatment. (b) SEM image showing the membrane damage formed on different *E. coli* surfaces after treatment at 2 V for 10 s. (c) Fluorescence microscopy images of *E. coli* without treatment. (d) Fluorescence microscopy images of *E. coli* after treatment at 2 V for 10 s. (e) The released DNA concentration of *E. coli* after treatment. (f) The electric field distribution with an applied voltage of 2 V of near the tip structure of CNT sponges (diameter, 10 nm; length, 1 μm) in water showing the enhancement of the electric field strength (the scale is 200 nm).

diameter.[33] By modifying the electrodes with tip structures that have high aspect ratios (*e.g.*, CNTs and nanowires), E_{tip} can be several orders of magnitude stronger than E_0.[33,34] Therefore, the CNTs can theoretically provide the same strength of electric field near the tip structure to achieve cell electroporation inactivation with a much lower applied voltage. The electric field simulation results also suggested that the electric field at the vicinity of CNT tip structure was above 10^7 V m^{-1} at an applied voltage of 2 V (Fig. 5f), which was strong enough for electroporation cell inactivation. In comparison, an electrode of same material but with a flat surface under the same conditions will produce an electric field of only ~10^4 V m^{-1}.

4. Conclusions

In summary, we have introduced a simple, scalable, controllable and binder and template free 3D CNT sponge using a self-expansion method. An EDC equipped with the as-prepared CNT sponges achieved superior cell inactivation performance (<0.00001% microbe survival rate indication no live microbe detection) with an extremely low applied voltage (2 V), trace energy consumption (20 J L^{-1}),and outstanding durability (>60 min). The CNT sponge EDC can be easily powered by batteries or solar cells and shows the best energy consumption performance among all the cell inactivation technologies reported to date. This technology will substantially change the current production methods of food and water industry, and also arouse interest in a wild range of promising guides for the extraction high value products from the cell and point-of-care devices for measuring small molecules to bring medical diagnostic devices closer to the patient.

Conflicts of interest

There are no conflicts to declare.

Acknowledgements

This study was supported by Key Program of the National Natural Science Foundation of China (No. 51138006), the National Key Research and Development Program of China for International Science & Innovation Cooperation Major Project between Governments (No. 2016YFE0118800), the National Basic Research Program of China (2012CB932301) and the NSFC (51472141). The Collaborative Innovation Center for Regional Environmental Quality also supported this research.

References

1 M. Ferrari, *Nat. Rev. Cancer*, 2005, **5**, 161–171.
2 X. Michalet, F. F. Pinaud, L. A. Bentolila, J. M. Tsay, S. Doose, J. J. Li, G. Sundaresan, A. M. Wu, S. S. Gambhir and S. Weiss, *Science*, 2005, **307**, 538–544.
3 X. Sun, L. Zhuang, K. Welsher, J. T. Robinson, A. Goodwin, S. Zaric and H. Dai, *Nano Res.*, 2008, **1**, 203–212.
4 Z. Guo, Y. Zou, H. He, J. Rao, S. Ji, X. Cui, H. Ke, Y. Deng, H. Yang and C. Chen, *Adv. Mater.*, 2016, **28**, 10155–10164.
5 C. T. White and T. N. Todorov, *Nature*, 2001, **411**, 649–651.
6 S. Berber, Y. K. Kwon and D. Tomanek, *Phys. Rev. Lett.*, 2000, **84**, 4613–4616.
7 S. Nardecchia, D. Carriazo, M. L. Ferrer, M. C. Gutierrez and F. D. Monte, *ChemInform*, 2013, **42**, 794–830.
8 X. Gui, J. Wei, K. Wang, A. Cao, H. Zhu, Y. Jia, Q. Shu and D. Wu, *Adv. Mater.*, 2010, **22**, 617–621.

9 M. B. Bryning, D. E. Milkie, M. F. Islam, L. A. Hough, J. M. Kikkawa and A. G. Yodh, *Adv. Mater.*, 2007, **19**, 661–664.
10 X. Gui, A. Cao, J. Wei, H. Li, Y. Jia, Z. Li, L. Fan, K. Wang, H. Zhu and D. Wu, *ACS Nano*, 2010, **4**, 2320–2326.
11 G. N. Ostojic, *ChemPhysChem*, 2012, **13**, 2102–2107.
12 X. Zhang, J. Liu, B. Xu, Y. Su and Y. Luo, *Carbon*, 2011, **49**, 1884–1893.
13 S. Luo, Y. Luo, H. Wu, M. Li, L. Yan, K. Jiang, L. Liu, Q. Li, S. Fan and J. Wang, *Adv. Mater.*, 2017, **29**, 1603549.
14 X. Xie, M. Ye, L. B. Hu, N. Liu, J. R. Mcdonough, C. Wei, H. N. Alshareef, C. S. Criddle and Y. Cui, *Energy Environ. Sci.*, 2012, **5**, 5265–5270.
15 D. F. Rodrigues and M. Elimelech, *Environ. Sci. Technol.*, 2010, **44**, 4583–4589.
16 D. Das, J. Plazastuttle, I. V. Sabaraya, S. S. Jain, T. Saboattwood and N. B. Saleh, *Environ. Sci.: Nano*, 2016, **4**, 60–68.
17 L. Wang, D. Zhu, J. Chen, Y. Chen and W. Chen, *Environ. Sci.: Nano*, 2017, **4**, 558–564.
18 Y. Xia, P. Yang, Y. Sun, Y. Wu, B. Mayers, B. Gates, Y. Yin, F. Kim and H. Yan, *Adv. Mater.*, 2003, **15**, 353–389.
19 X. Xie, W. Zhao, H. R. Lee, C. Liu, M. Ye, W. Xie, B. Cui, C. S. Criddle and Y. Cui, *ACS Nano*, 2014, **8**, 11958–11965.
20 K. K. Sakimoto, C. Liu, J. Lim and P. Yang, *Nano Lett.*, 2014, **14**, 5471–5476.
21 X. Xie, L. Hu, M. Pasta, G. F. Wells, D. Kong, C. S. Criddle and Y. Cui, *Nano Lett.*, 2011, **11**, 291–296.
22 C. Liu, X. Xie, W. Zhao, J. Yao, D. Kong, A. B. Boehm and Y. Cui, *Nano Lett.*, 2014, **14**, 5603–5608.
23 T. Kotnik, W. Frey, M. Sack, S. H. Meglič, M. Peterka and D. Miklavčič, *Trends Biotechnol.*, 2015, **33**, 480–488.
24 M. Shahini and J. T. Yeow, *Lab Chip*, 2013, **13**, 2585–2590.
25 C. Gusbeth, W. Frey, H. Volkmann, T. Schwartz and H. Bluhm, *Chemosphere*, 2009, **75**, 228–233.
26 G. Saldaña, I. Álvarez, S. Condón and J. Raso, *Crit. Rev. Food Sci. Nutr.*, 2014, **54**, 1415–1426.
27 H. Tang, T. Liu and P. Jiang, *J. Nanosci. Nanotechnol.*, 2013, **13**, 1385.
28 A. Joss, H. Siegrist and T. A. Ternes, *Water. Sci. Technol.*, 2008, **57**, 251–255.
29 C. Liu, X. Xie, W. Zhao, N. Liu, P. A. Maraccini, L. M. Sassoubre, A. B. Boehm and Y. Cui, *Nano Lett.*, 2013, **13**, 4288–4293.
30 D. T. Schoen, A. P. Schoen, L. Hu, H. S. Kim, S. C. Heilshorn and Y. Cui, *Nano Lett.*, 2010, **10**, 3628–3632.
31 Z. Y. Huo, X. Xie, T. Yu, Y. Lu, C. Feng and H. Y. Hu, *Environ. Sci. Technol.*, 2016, **50**, 7641–7649.
32 M. S. Rahaman, C. D. Vecitis and M. Elimelech, *Environ. Sci. Technol.*, 2012, **46**, 1556–1564.
33 R. Chapana, C. Duarte, Z. Ren, A. K. Kempa and M. Giersig, *Nano Lett.*, 2004, **4**, 985–988.
34 M. Poudineh, R. M. Mohamadi, A. Sage, L. Mahmoudian, E. H. Sargent and S. O. Kelley, *Lab Chip*, 2014, **14**, 1785–1790.